*Applied Biological Research* 25(4): 465-474; (2023)
DOI: 10.5958/0974-4517.2023.00054.X

# INNOVATIVE APPROACHES TO ENHANCE GASTRIC RETENTION OF RABEPRAZOLE USING *Macrocystis pyrifera* EXTRACT

Pynskhemlin Syiemlieh, K.S. Srilatha, Hindustan Abdul Ahad*, Chrishmitha Sequeira, Becare Dkhar, and John Mithi

*Department of Pharmaceutics, R.R College of Pharmacy, Bangalore – 560 090, Karnataka (India)*
*****e-mail: *abdulhindustan@mail.com*

(Received 14 August, 2023; accepted 13 October, 2023)

## ABSTRACT

**The work aimed to formulate and assess floating tablets of Rabeprazole (RBZ) for treating peptic ulcers. Effervescent tablets were produced (F1-F9) with variations in the concentration of synthetic polymer HPMC K15 for F1, F2, and F3; natural polymer *Macrocystis pyrifera* extract (sodium alginate) for F4, F5, and F6; and combinations of these polymers for F7, F8, and F9. The research involved several stages, including pre-formulation studies of the pure drug. The tablets were assessed for compatibility, pre-formulation, and post-formulation studies. The compatibility study indicated that there were no interfaces between drug and polymers. The floating tablets passed all the pre- and post-compression constraints. Among them, F6 exhibited a drug content of 99.67 ± 0.11% and sustained drug release over 8 h. All formulations displayed favorable floating behaviour and remained afloat for more than 24 h. The study concludes that a combination of synthetic (HPMC K15) and natural (*Macrocystis pyrifera* extract) polymers found to extend the RBZ residence time in the stomach and achieve sustained drug discharge. This approach could hold promise for improving the treatment of peptic ulcers.**

**Keywords:** Effervescent, floating, RBZ, sustained release, tablets, ulcer

## INTRODUCTION

Peptic ulcers, characterized by stomach or duodenal lining damage, stem from an imbalance between protective and aggressive factors in the gastric mucosa (Lanas and Chan, 2017). Endogenous defensive factors like mucus secretion and antioxidants interact with aggressive factors like acid and pepsin secretions, leading to ulcer development. Environmental factors like smoking, poor diet, alcohol consumption, NSAID use, and *H. pylori* infection contribute to the condition (Davis and Robson, 2016). This results in various symptoms including pain, early satiety, nausea, bloating, and more. Rabeprazole (RBZ), classified as a proton pump inhibitor (PPI), plays a crucial role in treating acid-related disorders like GERD and peptic ulcers. By covalently binding and inactivating the gastric proton pump, it effectively reduces gastric acid production, which in turn elevates gastric pH. This mechanism is particularly relevant in managing peptic ulcer disease, especially when combined with *H. pylori* eradication therapy. These drugs, including RBZ, are benzimidazole derivatives that need to concentrate in the acidic secretory canaliculus of parietal cells. They endure conversion to active sulfenamide compounds, allowing them to form covalent inhibitory bonds with specific cysteine residues on the active parietal cell proton pump (H+/K+-ATPase) (Pace and Pallota, 2007).

Floating drug delivery systems (FDDS) or hydro-dynamically balanced systems (HBS) are designed as low-density formulations that possess the inherent ability to float on gastric matters

within the stomach. This buoyant property enables them to prolonged time. This unique characteristic is particularly beneficial for the drugs that require sustained discharge and prolonged contact with the gastric mucosa (Kousar and Ahad, 2022). The primary objective of an FDDS is to discharge the drug component at a controlled rate while it remains afloat over gastric matters. This not only contributes to the increased gastro-retention time but also helps in reducing the fluctuations in drug concentration that can occur due to the movement of gastrointestinal matters. By keeping the drug in stomach for an extended period, FDDS can enhance drug absorption and optimize its therapeutic effects (Chinthaginjala and Barghav, 2019). In essence, FDDS represents a gastro-retentive drug delivery system (GRDDS) that serves to control the pharmacokinetic discharge rate of a drug, ensuring that it reaches and remains at a specific site within the gastrointestinal tract for an extended period (Chinthaginjala and Ahad, 2021). This controlled discharge mechanism is crucial for achieving the desired pharmacological action of drug. Since RBZ is highly soluble and has a short half-life of 1-2 h, the objective of present study was to develop FDDS for RBZ to increase gastric retention time and sustain RBZ release, so as to enhance the treatment of peptic ulcer disease. Specific objectives included the formulation of FDDS, conducting *in vitro* characterization, assessing pharmacokinetics, evaluating *in vivo* efficacy, comparing it to conventional RBZ, ensuring safety and tolerability, and optimizing for potential clinical use. This research was intended to improve peptic ulcer management by prolonging the drug release and enhancing therapeutic effects through controlled delivery.

## MATERIALS AND METHODS

Rabeprazole (RBZ) was procured from Yarrow Chem Products, India whereas HPMC K15 was obtained from Balaji Drugs. *Macrocystis pyrifera* extract (sodium alginate), lactose, sodium bicarbonate, and citric acid were obtained from SD Fine Chemicals, India while magnesium stearate was sourced from Thomas Baker. All the chemicals used in the study were of analytical grade.

### *Pre-formulation studies*

The solubility of RBZ was assessed by using different solvents, namely water, alcohol, 0.1N HCl, n-hexane, and ethyl acetate (Kohli and Patil, 2018). Thiele's tube apparatus was utilized to ascertain the melting point of RBZ. The drug was loaded into a capillary tube that was sealed at one end, and the temperature at which it melted was evaluated with the aid of a thermometer (Young, 2013). The $\lambda_{max}$ of RBZ was determined using a UV double-beam spectrophotometer (Shimadzu 1800) in the range of 200-400 nm. A stock solution of RBZ in 0.1N HCl at a concentration of 100 μg $mL^{-1}$ was used for this purpose (Gul and Basheer, 2017). A stock solution of RBZ (100 μg $mL^{-1}$) was prepared using 0.1N HCl. Subsequently, the solutions ranging from 5 to 25 μg $mL^{-1}$ were created by diluting the stock solution with 0.1N HCl. The absorbance of each solution was determined by using a UV double-beam spectrophotometer at 274 nm (Giriraj and Sivakkumar, 2014). To assess the compatibility between drug and polymers utilized in formulation, a compatibility study was conducted. This involved subjecting both the drug alone and drug-polymer combinations to FTIR spectroscopy (Type II Alpha). The range for scanning was 400-4000 $cm^{-1}$ and the resolution was 4 $cm^{-1}$ (Gunji and Nadendla, 2012).

### *Pre-compression evaluation*

The powder blends of the formulations were analysed to determine their bulk and tapped density. These measurements were then used to estimate the compressibility index and Hausner's ratio (Asija and Asija, 2015), which provided insights into their flow properties. The flow characteristics of powder blend were evaluated through the determination of the angle of repose (Annepogu and Ahad, 2020).

### *Preparation of RBZ floating tablets*

The floating tablets (FTs) containing RBZ were established through the direct compression technique (Goyal and Dubey, 2015). This process involved the utilization of synthetic polymer (HPMC K15),

natural polymer (*Macrocystis pyrifera* extract), and their combination, in addition to sodium bicarbonate and citric acid. Precise controls of each component were taken and passed through 22 mesh size (Chinthaginjala and Ahad, 2021). All the constituents, except magnesium stearate, were meticulously blended using a glass mortar to achieve uniform amalgamation (Rajora and Nagpal, 2022). After achieving sufficient homogeneity of drug and excipients, magnesium stearate was incorporated as a post-lubricant and mixed for 2-3 min. Following this, rotary tablet machines were employed to compact the mixture into tablet form as given under:

| Ingredients (mg) | F1 | F2 | F3 | F4 | F5 | F6 | F7 | F8 | F9 |
|---|---|---|---|---|---|---|---|---|---|
| Rabeprazole | 20 | 20 | 20 | 20 | 20 | 20 | 20 | 20 | 20 |
| HPMC K15 | 100 | 110 | 120 | - | - | - | 50 | 55 | 60 |
| *Macrocystis pyrifera* extract | - | - | - | 100 | 110 | 120 | 50 | 55 | 60 |
| Lactose | 39.67 | 29.67 | 19.67 | 39.67 | 29.67 | 19.67 | 39.67 | 29.67 | 19.67 |
| Sodium bicarbonate | 62.5 | 62.5 | 62.5 | 62.5 | 62.5 | 62.5 | 62.5 | 62.5 | 62.5 |
| Citric acid | 20.83 | 20.83 | 20.83 | 20.83 | 20.83 | 20.83 | 20.83 | 20.83 | 20.83 |
| Talc | 4 | 4 | 4 | 4 | 4 | 4 | 4 | 4 | 4 |
| Magnesium stearate | 3 | 3 | 3 | 3 | 3 | 3 | 3 | 3 | 3 |

***Post-compression evaluation***

Tablet hardness, which measures the resistance of tablets to breakage, was evaluated using a Pfizer hardness tester (J.K. Scientific CO.). The hardness value (kg $cm^{-2}$), gauges the tablets' mechanical strength and their ability to withstand handling and stress during manufacturing, packaging, and transportation (Nakamura and Fukai, 2021). As part of quality control measures, a sample of 20 tablets was taken from each batch. Each tablet within this sample was individually weighed to find whether there was any significant weight variation among the tablets in the batch. This process helps to ensure the uniformity and consistency of the tablets' weight, which is a crucial factor in their performance and effectiveness (Ahad and Rajesh, 2010). For assessing the friability, 10 tablets were precisely weighed and then subjected to a friability test using a friability test apparatus (Roche friabilator) (Kukati and Chittimalli, 2014). During the test, the FTs were revolved at 25 rpm for 4 min. After the rotation, the tablets were carefully removed, freed from dust, and weighed once again (Ahad and Kumar, 2009). The friability of tablets is a measure of their tendency to undergo abrasion or damage during handling and transportation. It's an important quality parameter as it indicates the tablet's physical integrity. Generally, the friability values that fall below 1% are considered acceptable in pharmaceutical manufacturing. The friability was considered as % weight loss of tablets due to the abrasion during test. The formula used for this calculation takes into account the initial tablet weight and the post-test weight after removing the dust. This deviousness provides insight into the tablet's ability to withstand mechanical stress, contributing to their overall quality and effectiveness (eq. 1).

$$\% \text{ Friability } = \frac{W1 - W2}{W1} X100 \text{ ---------- (eq. 1)}$$

Where, $W_1$ = initial weight of the tablets, $W_2$ = final weight of the tablets

The finding of tablet thickness is crucial to ensure consistent tablet size. To assess this parameter, three tablets were erratically chosen, and their thickness was assessed with Vernier Caliper (Mitutoyo 500-197-20). This process helps to maintain the uniformity in tablet dimensions, contributing to the overall quality and appearance of tablets (Ahad and Kumar, 2011). To assess the RBZ content, 5 tablets were individually weighed and powdered. The amount of powder equivalent to the average weight of tablets was carefully assessed. This powder was then subjected to extraction in 0.1N HCl to dissolve the drug. The drug matter in the solution was assessed by assessing the absorbance at 274 nm (García-Torres and De La Mora, 2023), after appropriate dilution, with a UV double-beam spectrophotometer (Pattanayak and Sharma, 2007). This procedure helps to ascertain the actual drug matter within the tablets, ensuring their quality and consistency.

To determine the floating lag time and floating time, the testing procedure involved immersing a tablet in a 100 mL beaker containing a solution of 0.1N HCl. This setup serves to evaluate the tablet's

interaction with the liquid medium. The "floating lag time" stands as a crucial metric, representing the time span between introducing the tablet into the solution and the point at which it ascends to the liquid's surface. This parameter serves as an indicator of the tablet's promptness in achieving buoyancy, reflecting its initial responsiveness to the surrounding conditions (Oladeji and Dadou., 2022). The assessment encompasses the "Total Floating Time (TFT)," which encompasses the entire duration the tablet remains afloat on the surface of liquid. This duration is an essential measure of the tablet's capacity to maintain its buoyant state throughout its anticipated period of utilization (Vinod and Chetankumar, 2022). A prolonged TFT indicates a tablet's ability to sustain its buoyancy over an extended time frame, which can be critical in scenarios where extended floating time is required. By evaluating both the floating lag time and TFT, this testing procedure provides valuable insights into the tablet's performance, design, and its suitability for applications demanding controlled floating behaviour.

The swelling index of tablet was assessed with 0.1N HCl at room temperature (Mundarinti and Ahad, 2023). The tablet's weight after swelling was found out at specific time intervals (eq. 2).

$$\text{Swelling index} = \frac{W1 - W0}{W0} X100 \text{ ---------- (eq. 2)}$$

Where, $W_1$: weight of tablet at time t; $W_0$: Initial weight of tablet.

***In vitro drug discharge studies***

The drug discharge from the FTs was evaluated through a dissolution test by a USP type II dissolution apparatus (LAB India) with a paddle configuration. The test was conducted at a temperature of 37 ± 0.5°C with a paddle rotation speed of 50 rpm. The dissolution medium used was 900 mL of 0.1N HCl (Shwetha and Kamath, 2012). During the test, 5 mL samples were withdrawn from the dissolution apparatus at specified time intervals, and these samples were immediately replaced with fresh dissolution media. The withdrawn samples were then filtered and, if necessary, appropriately diluted. The absorbance of these solutions were judged at 274 nm by a UV spectrophotometer. This methodology enables the quantification of RBZ discharged from FTs over time, providing the valuable information about the discharge kinetics and performance of tablets.

## RESULTS AND DISCUSSION

***Pre-formulation***

The organoleptic characteristic holds significance due to the inclusion of organoleptic property assessment, which serves as an initial assessment for any drug. The pure RBZ was a slightly yellowish solid with a distinct odour, emphasizing the importance of evaluating the sensory characteristics of pharmaceutical substances. Solubility studies revealed that RBZ exhibited solubility in water, ethanol, and 0.1N HCl. However, it was insoluble in n-hexane and ethyl acetate. These findings provide valuable insights into the drug's dissolution behaviour and potential interactions with different types of solvents. The melting point conducted by Thiele's tube method proved the drug's characteristics. The average melting point was 139.33 ± 1.15°C. The observed sharp melting point of the RBZ sample holds significance in confirming the drug's identity and purity. Its alignment with the specified value in the official monograph underscores the reliability of the received drug sample and ensures its high quality and consistency.

***$\lambda_{max}$ determination and compatibility by FTIR***

The assessment of $\lambda_{max}$ of RBZ was conducted in 0.1 N HCl. The $\lambda_{max}$ value of RBZ in 0.1 N HCl was assessed to be 274 nm. This specific wavelength is crucial for subsequent spectroscopic analyses and quantification of the RBZ's concentration in solution (Fig. 1). A standard calibration curve was constructed, plotting concentration (µg $mL^{-1}$) against absorbance.

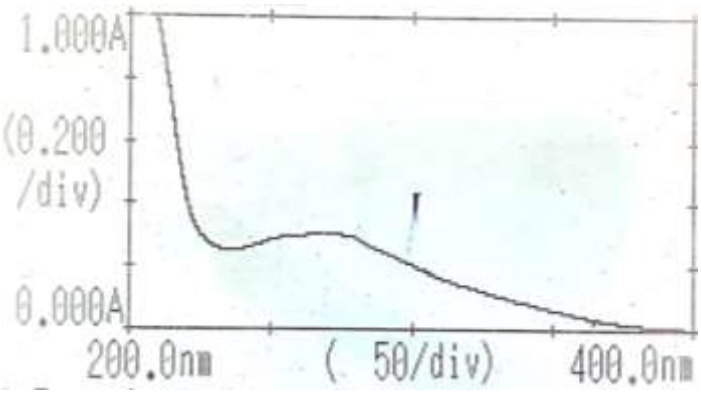


**Fig. 1: $\lambda_{max}$ of RBZ by UV spectrophotometer**

The regression equation derived from the curve was y = 0.0312x + 0.0009, with a high regression coefficient value of $r^2$ = 0.999. This regression coefficient allowed for the calculation of % cumulative drug release (%CDR). The conformity of standard calibration curve to Beer's law was evident as an increase in concentration corresponded to a proportional increase in absorbance (Fig. 3A). To assess potential interactions between the RBZ and polymers in the formulation, RBZ and polymer compatibility studies were conducted by the FTIR technique, the analysis aimed to find if there were any chemical interactions between the components. The FTIR spectrum of pure RBZ displayed its characteristic absorption peaks. This approach helps to ensure that the RBZ and polymers maintain their integrity and individual characteristics within the formulation. Fig. 2 depicts the comparison between pure RBZ and RBZ with added excipients. This visual representation offers an overlay of spectral characteristics, allowing for an assessment of any potential shifts or alterations in the RBZ's signature peaks due to the presence of the excipients. Such analyses are crucial to confirming the compatibility of the RBZ with the selected formulation components and ensuring the integrity of the RBZ within the final product. The FTIR analysis indicated that there was no interaction between the drug and polymers. The characteristic peaks and stretches of drug remained unaffected within drug-polymers combination, confirming the compatibility of these components and supporting the stability of formulation.

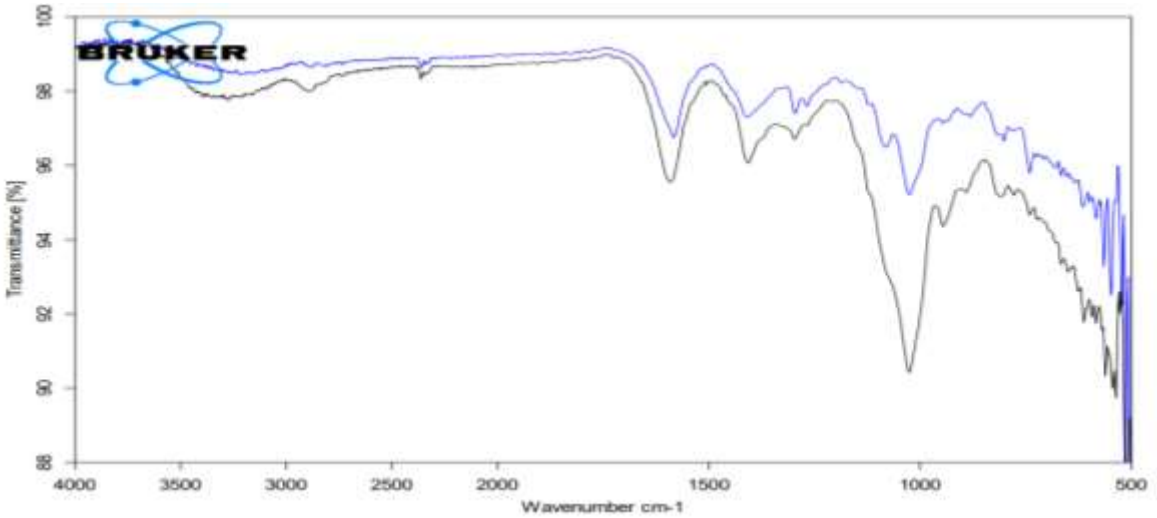


**Fig. 2: FTIR spectra of pure RBZ (blue coloured) and RBZ excipients blend (Black) (coloured)**

***Pre-compression studies***

The angle of repose was assessed for all formulations (F1-F9), yielding values ranging from 32.47 ± 1.67 to 39.38 ± 1.37°. The values were below 40°, indicates good flow properties across the formulations. Bulk density and tapped density assessments were conducted across formulations (F1-F9). The bulk density ranged from 0.425 ± 0.02 to 0.519 ± 0.03 g $cm^{-3}$, while the tapped density varied between 0.497 ± 0.01 and 0.614 ± 0.05 g $cm^{-3}$. Carr's index evaluation for formulations revealed values within the range of 12.18 ± 0.43 to 19.54 ± 0.64%. Hausner's ratio ranged within the scope of

1.12 ± 0.02 to 1.23 ± 0.07 (Table 1). The observed positive outcomes in terms of flow characteristics, compressibility, and Hausner's ratio across formulations F1 to F9 underscore their suitability for tablet formulation. These parameters collectively ensure the production of tablets with consistent quality, which is essential for effective pharmaceutical manufacturing and reliable delivery of medications.

**Table 1: Pre-compression flow characteristics of powder blends**

| Formulation | Angle of repose (º) | Bulk density (g $mL^{-1}$) | Tapped density (g $mL^{-1}$) | Carr's index (%) | Hausner's ratio |
|---|---|---|---|---|---|
| F1 | 32.47 ± 1.67 | 0.436 ± 0.05 | 0.522 ± 0.02 | 16.57 ± 0.12 | 1.19 ± 0.07 |
| F2 | 34.92 ± 1.01 | 0.462 ± 0.02 | 0.522 ± 0.01 | 12.18 ± 0.43 | 1.12 ± 0.02 |
| F3 | 35.81 ± 1.59 | 0.425 ± 0.02 | 0.497 ± 0.01 | 15.15 ± 2.15 | 1.17 ± 0.03 |
| F4 | 36.38 ± 0.67 | 0.467 ± 0.03 | 0.578 ± 0.04 | 19.09 ± 1.27 | 1.21 ± 0.01 |
| F5 | 33.67 ± 0.14 | 0.519 ± 0.03 | 0.614 ± 0.05 | 15.37 ± 1.96 | 1.18 ± 0.08 |
| F6 | 37.78 ± 0.78 | 0.483 ± 0.03 | 0.600 ± 0.02 | 19.48 ± 0.58 | 1.23 ± 0.07 |
| F7 | 39.06 ± 2.25 | 0.471 ± 0.02 | 0.552 ± 0.02 | 14.56 ± 0.55 | 1.16 ± 0.07 |
| F8 | 39.38 ± 1.37 | 0.478 ± 0.03 | 0.594 ± 0.05 | 19.54 ± 0.64 | 1.20 ± 0.03 |
| F9 | 36.65 ± 1.27 | 0.484 ± 0.04 | 0.585 ± 0.04 | 17.11± 4.08 | 1.20 ± 0.06 |

Values in mean ± SD

***Post-compression***

The tablets that were prepared underwent an evaluation for hardness. Across all formulations, the hardness fell within the range of 5.76 ± 0.11 to 9.73 ± 0.11 kg $cm^{-2}$. These results signify that the tablets possessed satisfactory mechanical strength, a crucial factor ensuring their resilience and integrity during handling and usage. The tablets weight across the formulations ranged from 0.24 ± 0.01 to 0.25 ± 0.01 mg. The weight variation test indicated that all tablets met the acceptable criteria, as the % weight variation fell within the prescribed limits of ± 7.5% of the specified weight, as outlined in the Indian Pharmacopoeia (Kohli and Patil, 2018). Friability values spanned from 0.75 ± 0.16 to 0.83 ± 0.17%, values below 1% indicate that the tablets exhibited minimal abrasion or damage during the testing process, emphasizing their ability to withstand mechanical stress and maintain their structural integrity. The evaluation of formulated tablets for thickness was consistently observed to be around 4 mm across all formulations. Thickness remained uniform across the various formulations tested. The uniformity in tablet thickness signifies a controlled and consistent manufacturing process, ensuring that each tablet maintains the desired dimensions.

The evaluation of floating lag time was conducted across all formulations (F1 to F9) using 0.1N HCl. The floating lag time varied from 16.66 ± 0.57 to 76.66 ± 1.15 sec. This parameter signifies the duration the tablet takes to initiate floating on the surface of the dissolution medium, showing its buoyancy and capacity to remain suspended. The floating lag time, as determined in this study, represents the interval required for the tablets to begin floating on the surface of the dissolution medium. This parameter serves as an indicator of the tablets' buoyancy and their ability to remain afloat, which is crucial for their intended function. Remarkably, the formulations exhibited impressive capability to remain buoyant for a duration surpassing 20 h. This extended floating behaviour holds significant implications, primarily related to the potential to prolong the time the tablets spend in the stomach. By doing so, these formulations can effectively enhance the residence time of drug within the gastric environment. This, in turn, facilitates the sustained discharge of the drug, contributing to its therapeutic impact over an extended period.

The capacity of these formulations to maintain their floating properties for such an extended duration showcases their promising potential as GRDDS. Such systems can address challenges associated with drug absorption and therapeutic efficacy, offering an innovative approach to optimize drug discharge patterns and improve patient outcomes (Vantimitta and Jeganath, 2022). The determined drug matter within the prepared formulations serves as an indicator of their ability to consistently deliver the intended drug dosage. Notably, among the investigated formulations, F6

stands out for having the most optimal drug matter. This finding underscores the reliability of F6 in maintaining the targeted drug concentration, which is pivotal for achieving the desired therapeutic outcomes and ensuring patient safety and efficacy.

The swelling index of the prepared tablet formulations (F1-F9) showed a significant degree of swelling, with highest degree of swelling in formulation F4, lowest in formulation F1 (Fig. 3B). The observed variations in swelling index underscores the formulation-specific distinctions in water absorption and subsequent tablet expansion (Kadam and Upadhye, 2014). These differences can play a role in influencing the discharge kinetics of the drug as well as the overall performance of the tablets in terms of their therapeutic effectiveness.

**Table 2: Post-compression characteristics of formulated tablets**

| Formulation | Hardness (kg $cm^{-2}$) | Weight variation (%) | Thickness (mm) | Friability (%) | Floating lag time (sec) | Floating time (h) | RBZ content |
|---|---|---|---|---|---|---|---|
| F1 | 6.83 ± 0.57 | 0.25 ± 0.01 | 4.00 ± 0.23 | 0.80 ± 0.12 | 19.00 ± 0.02 | 22.21 ± 0.25 | 92.58 ± 2.16 |
| F2 | 9.45 ± 0.24 | 0.25 ± 0.01 | 4.04 ± 0.18 | 0.82 ± 0.05 | 19.33 ± 0.57 | 20.35 ± 0.51 | 95.06 ± 3.15 |
| F3 | 9.73 ± 0.11 | 0.24 ± 0.01 | 4.03 ± 0.17 | 0.77 ± 0.82 | 16.66 ± 0.57 | 21.21 ± 0.84 | 90.05 ± 5.12 |
| F4 | 7.86 ± 0.46 | 0.25 ± 0.01 | 4.03 ± 0.01 | 0.82 ± 0.16 | 76.66 ± 1.15 | 22.18 ± 0.45 | 91.31 ± 4.25 |
| F5 | 7.46 ± 0.57 | 0.23 ± 0.02 | 4.02 ±.0.11 | 0.83 ± 0.05 | 44.66 ± 0.57 | 20.75 ± 0.96 | 98.13 ± 6.14 |
| F6 | 9.13 ± 0.41 | 0.23 ± 0.01 | 4.01 ± 0.37 | 0.79 ± 0.11 | 49.33 ± 0.57 | 22.94 ± 0.84 | 99.67 ± 0.11 |
| F7 | 9.53 ± 0.37 | 0.25 ± 0.01 | 4.02 ± 0.33 | 0.79 ± 0.22 | 46.33 ± 1.15 | 23.56 ± 1.25 | 93.21 ± 2.17 |
| F8 | 8.24 ± 0.91 | 0.23 ± 0.01 | 4.01 ± 0.05 | 0.75 ± 0.16 | 58.66 ± 1.15 | 21.52 ± 0.85 | 97.43 ± 3.2 |
| F9 | 5.76 ± 0.11 | 0.24 ± 0.01 | 4.00 ± 0.04 | 0.83 ± 0.17 | 51.66 ± 0.57 | 20.02 ± 0.36 | 97.36 ± 2.17 |

Mean ± SD; n = 3

***In vitro RBZ discharge***

The formulated tablets contain RBZ within the range of 90.05 ± 5.12 to 99.67 ± 0.11%. The formulation F6 exhibited the highest RBZ content among the tested formulations (Table 2). The behaviour of floating RBZ tablets encompassed *in vitro* RBZ release studies over an 8 h in a 0.1N HCl solution. Throughout this duration, the tablets were immersed in solution, allowing the measurement of RBZ release at regular intervals. The corresponding RBZ discharge profiles revealed distinct variations among the formulations: F1 exhibited an RBZ release of 50.2 ± 1.99%, F2 released 45.2 ± 2.24%, F3 displayed 49.5 ± 0.19%, F4 demonstrated 33.9 ± 0.98%, F5 showcased 32.7 ± 0.23%, F6 presented 30.41 ± 1.2%, F7 indicated 40.4 ± 1.14%, F8 manifested 32.7 ± 0.72%, and F9 unveiled 39.3 ± 0.84% (Fig. 3C). These profiles show diverse rates of RBZ release from each formulation, imparting valuable insights into their dissolution kinetics and potential therapeutic effectiveness. The *in vitro* discharge studies unveiled distinct drug discharge behaviours among the different formulations. This observation highlights the variations in drug discharge rates and extents within the various formulations over the designated 8 h timeframe. Such findings emphasize the significance of formulation composition and design in determining the drug discharge kinetics and overall performance. According to the Korsmeyer-Peppas plot, all the formulations displayed a super case II transport mechanism (Paarakh and Jose, 2018), as indicated by n values ranging from 0.9523 to 1.3199. These outcomes elucidate the underlying discharge dynamics and mechanisms of drug from each formulation, providing valuable insights for optimizing drug delivery strategies.

***Kinetic studies***

Kinetic discharge for formulations (F1-F9) (Fig. 3D, E, and F), reveals their respective discharge mechanisms. All formulations exhibited adherence to Zero-order kinetics, with $r^2$ values spanning from 0.8029 to 0.9931 (Table 3). Additionally, formulations conformed to the Higuchi model, signifying a rate diffusion-controlled mechanism (Paarakh and Jose, 2018). The $r^2$ values ranged from 0.7830 to 0.9741.

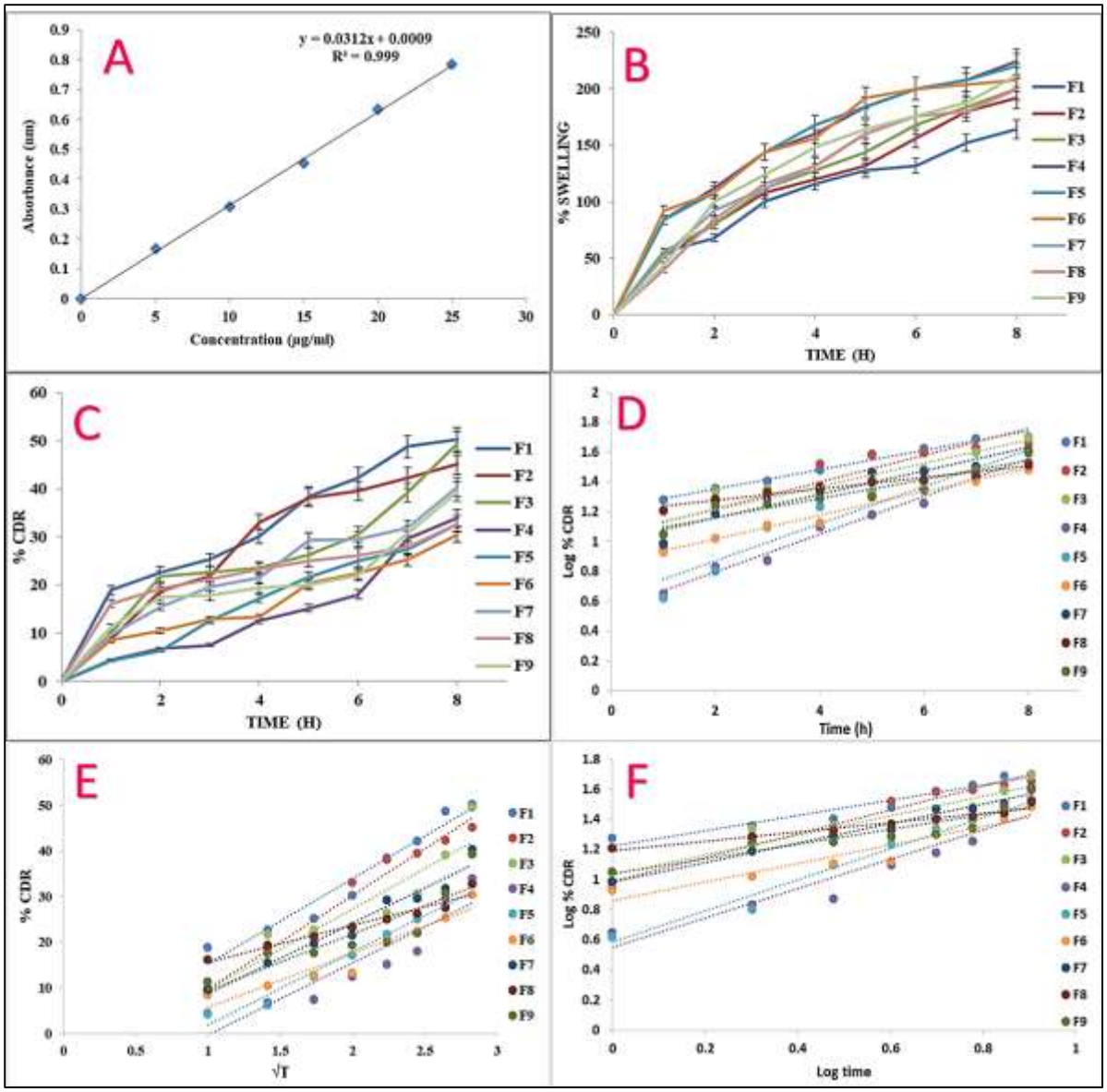


**Fig. 3: Calibration curve of RBZ in 0.1 N HCl (A); Swelling index of FTs of RBZ (B); *In vitro* RBZ discharge (C); First order kinetics (D); Higuchi model (E); and Korsmeyer-Peppas plot (F)**

**Table 3: Kinetic discharge values of formulated tablets**

| Formulation | Mechanism of discharge | | | | |
|---|---|---|---|---|---|
| | Zero-order | First order | Higuchi | Korsmeyer-Peppas | |
| | $r^2$ | $r^2$ | $r^2$ | $r^2$ | Slope (n) |
| F1 | 0.9435 | 0.5776 | 0.9741 | 0.5813 | 1.1661 |
| F2 | 0.9416 | 0.6725 | 0.9627 | 0.7293 | 1.3199 |
| F3 | 0.9217 | 0.6443 | 0.9009 | 0.6664 | 1.2034 |
| F4 | 0.9322 | 0.8902 | 0.7830 | 0.8645 | 1.2738 |
| F5 | 0.9931 | 0.8427 | 0.9102 | 0.8869 | 1.3526 |
| F6 | 0.9654 | 0.7077 | 0.9265 | 0.6986 | 1.0820 |
| F7 | 0.9582 | 0.6618 | 0.9613 | 0.6883 | 1.1791 |
| F8 | 0.8029 | 0.4849 | 0.9562 | 0.4954 | 0.9523 |
| F9 | 0.8775 | 0.6059 | 0.8721 | 0.6020 | 1.0509 |

**Conclusion:** The floating tablets of rabeprazole (RBZ) were developed and evaluated for treating peptic ulcers using an effervescent system that employed sodium bicarbonate and citric acid as gas-generating agents. The tablets were prepared using a direct compression method and included synthetic polymer HPMC K15, natural polymer (*Macrocystis pyrifera* extract), and their combinations at varying concentrations. Among the tablet formulations, F6 which contained *Macrocystis pyrifera* extract (48% w/w), showcased sustained release over 8 h and holds good RBZ content, making it the optimal formulation. These tablets offer the potential to extend the gastric residence time and provide sustained drug discharge.

## REFERENCES


Ahad, H.A., Kumar, B.P., Haranath, C. and Reddy, K.S. 2009. Fabrication and evaluation of glimepiride *Cordia dichotoma* G. Forst fruit mucilage sustained release matrix tablets. *International Journal of Chemical Sciences,* **7**: 2555-2560.

Ahad, H.A., Kumar, C.S., Budideti, K.K.R., Battula, S.P. and Ayyavala, C.S. 2011. Formulation and evaluation of *Ficus glomerata* mucilage sustained release matrix tablets of gliclazide. *Pakistan Journal of Pharmaceutical Sciences,* **24**: 399-404.

Ahad, H.A., Rajesh, V., Gupta, M., Lasya, D., Harish, N. and Khamartaz, M. 2010. Fabrication and *in vitro* evaluation of *Glimepiride hibiscus esculentus* fruit mucilage sustained release matrix tablets. *International Journal of PharmTech Research,* **2**: 78-83,

Annepogu, H., Ahad, H.A. and Nayakanti, D. 2020. Determining the best poloxamer carrier for thiocolchicoside solid dispersions. *Turkish Journal of Pharmaceutical Sciences*, **17**: 372-380.

Chinthaginjala, H., Ahad, H.A., Bhargav, E. and Pradeepkumar, B. 2021. Central composite design aided formulation development and optimization of clarythromycin extended-release tablets. *Indian Journal of Pharmaceutical Education & Research*, **55**: 395-406.

Chinthaginjala, H., Ahad, H.A., Pradeepkumar, B., Gandhi, K.S., Kalpana, K., Pushpalatha, G. and Sumala, K. 2021. Formulation and *in vitro* evaluation of gastroretentive ofloxacin floating tablets using natural polymers. *Research Journal of Pharmacy and Technology,* **14**: 851-856.

Chinthaginjala, H., Barghav, G.C., Reddy, C.M., Pradeepkumar, B., Ahad, H.A., Akbari, B. and Shastry, C. 2019. Formulation and *in vitro* evaluation of floating tablets of dicloxacillin sodium using different polymers. *Journal of Young Pharmacists*, **11**: 247-253.

Davis, A. and Robson, J. 2016. The dangers of NSAIDs: Look both ways. *British Journal of General Practice*, **66**: 172-173.

García-Torres, I., De la Mora-De la Mora, I., López-Velázquez, G., Cabrera, N., Flores-López, L.A., Becker, I. and Enríquez-Flores, S. 2023. Repurposing of rabeprazole as an anti-*Trypanosoma cruzi* drug that targets cellular triosephosphate isomerase. *Journal of Enzyme Inhibition and Medicinal Chemistry,* **38**: 1-16. [*https://doi.org/10.1080/14756366.2023.2231169*].

Giriraj, P. and Sivakkumar, T. 2014. New simple spectrophotometric method for the simultaneous estimation of paracetamol and flupirtine maleate in pure and pharmaceutical dosage form. *International Journal of Spectroscopy*, **2014**: 1-6. [*https://doi.org/10.1155/2014/968420*].

Gul, S. and Basheer, S. 2017. UV visible spectrophotometric determination, validation and *in vitro* interaction of rabeprazole with chlorazepate. *Saudi Journal of Medical and Pharmaceutical Sciences*, **3**: 813-817.

Gunji, R., Nadendla, R.R. and Ponnuru, V.S. 2012. Simultaneous UV-spectrophotometric determination and validation of diclofenac sodium and rabeprazole sodium using hydrotropic agents in its tablet dosage form. *International Journal of Drug Development and Research,* **4**: 316-324.

Kadam, A.M., Upadhye, S., Honmane, S., Patil, S. and Patil, S. 2014. Formulation and evaluation of anti-ulcer floating tablet using swellable polymers. *International Journal of Drug Delivery*, **6**: 244-253.

Kousar, S., Ahad, H.A., Chinthaginjala, H., Babafakruddin, P., Lakunde, J. and Tarun, K. 2022. Gas generating floating tablets: A quick literature review for the scholars. *Asian Journal of Research in Chemistry*, **15**: 171-175.

Kukati, L., Chittimalli, K. and Shaik, N.B. 2014. Formulation and evaluation of floating tablets of cefpodoxime proxetil. *Journal of Scientific Research*, **6**: 563-579.

Lanas, A. and Chan, F.K. 2017. Peptic ulcer disease. *The Lancet*, **390**: 613-624.

Mundarinti, S.H.B. and Ahad, H.A. 2023. Impact of *Pistacia lentiscus* plant gum on particle size and swelling index in central composite designed amoxycillin trihydrate mucoadhesive microspheres. *Indian Journal of Pharmaceutical Education and Research,* **57**: 763-772.

Nakamura, S., Fukai, T. and Sakamoto, T. 2021. Orally disintegrating tablet manufacture via direct powder compression using cellulose nanofiber as a functional additive. *Aaps Pharmscitech*,**23**: 37-42.

Oladeji, S.A., Dadou, S.M., Zhao, M., Li, S., Jones, D.S. and Andrews, G.P. 2022. The development and optimisation of gastro-retentive floating tablets using fused deposition modelling 3D printing. *Journal of Pharmacy and Pharmacology*, **74**: 1450-1466.

Pace, F., Pallotta, S., Casalini, S. and Porro, G.B. 2007. A review of rabeprazole in the treatment of acid-related diseases. *Therapeutics and Clinical Risk Management*, **3**: 363-379.

Paarakh, M.P., Jose, P.A, Setty, C.M. and Peterchristoper, G.V. 2018. Release kinetics - Concepts and applications. *International Journal of Pharmacy Research & Technology*, **8**: 12-20.

Pattanayak, P., Sharma, R. and Chaturvedi, S. 2007. Simultaneous spectrophotometric estimation of rabeprazole sodium and itopride HCl. *Analytical Letters*, **40**: 2288-2294.

Rajora, A. and Nagpal, K. 2022. A critical review on floating tablets as a tool for achieving better gastric retention. *Critical Reviews™ in Therapeutic Drug Carrier Systems,* **39**: 65-103.

Shwetha, S., Kamath, K. and Kumar, S. 2012. Design and evaluation of floating microspheres of Rabeprazole sodium. *International Journal of Pharmacy and Pharmaceutical Sciences*, **4**: 104-120.

Smita, N., Sanidhya, S. and Bhaskar, V. 2016. Formulation and evaluation of Raloxifene hydrochloride tablets with improved dissolution profile. *International Journal of Advances in Pharmaceutics*, **5**: 127-139

Vantimitta, S.R. and Jeganath, S. 2022. Novel approaches of gastro retentive drug delivery system: A review. *International Journal of Health Sciences*, **6**: 3464-3476.

Vinod, M., Chetankumar, M., Bote, S. and Kolageri, S. 2022. Formulation and evaluation of floating tablets of pantoprazole. *Journal of Drug Delivery and Therapeutics*, **12**: 34-45.

Young, J. 2013. True melting point determination. *The Chemical Educator*, **18**: 203-208.